Fast Magnetic Reconnection Associated With Kink Modes

Keizo FUJIMOTO[1)] and Richard D. SYDORA[2)]

[1)] *Solar-Terrestrial Environment Laboratory, Nagoya University, Nagoya, Aichi 464-8601, Japan*
[2)] *Department of Physics, University of Alberta, Edmonton, Alberta T6G 2G7, Canada*

(Received: 28 August 2008 / Accepted: 21 October 2008)

A three-dimensional particle-in-cell simulation in a large system demonstrates that a kink mode significantly contributes to a fast reconnection by providing magnetic dissipation through anomalous resistivity. The anomalous resistivity is generated due to the electron heating in the thin electron current sheet. It is interesting that, although the kink mode broadens the width of the current sheet and decreases the inertia resistivity, the anomalous resistivity compensates the depletion so as to keep a high reconnection rate. The present result suggests that the electron dynamics in the electron diffusion region is automatically adjusted so as to produce sufficient dissipation for the fast magnetic reconnection.

Keywords: magnetic reconnection, particle-in-cell simulation, anomalous resistivity

1. Introduction

Magnetic reconnection is one of the key processes playing an important role in space and laboratory plasmas, by facilitating the fast conversion of energy stored in a compressed magnetic field into plasma kinetic energy. Although the explosive energy release associated with magnetospheric substorms and solar flares is known to persist for a few minutes to a few hours [1, 2], the magnetic dissipation mechanism supporting the steady-state fast reconnection is not yet established. The magnetic dissipation takes place in a microscopic region, so-called the diffusion region, where the ideal magnetohydrodynamic (MHD) constraints break down. In collisionless plasmas consisting of electrons and ions, the electron diffusion region develops in the vicinity of the magntic X-line, in which the electrons become unmagnetized so that the electron dynamics makes a significant impact on the magnetic dissipation. The electrons are strongly accelerated due to the reconnection electric field in the direction of the current density, and are ejected from the electron diffusion region as a consequence of the meandering/Speiser motion. Since the electrons carry away the energy gained by the electric field, this motion gives rise to the electrical resistivity, so-called the inertia resistivity [3, 4]. The effect is reduced to the gradient term of the electron pressure tensor $\boldsymbol{P}_e$ and the electron inertia term in the generalized Ohm's law [5]

$$-E_y = \frac{1}{n_e e}(\nabla \cdot \boldsymbol{P}_e)_y + \frac{m_e}{e}\frac{dV_{ey}}{dt}, \tag{1}$$

where $\boldsymbol{V}_e$ is the electron bulk velocity.

In order for the electron inertia resistivity to be large enough for the fast reconnection, the electron diffusion region has to be compact so as to keep the electron transit time short. It has been suggested that the compact electron diffusion region is guaranteed by a Hall effect invoked outside the electron diffusion region [6]. However, recent two-dimensional (2D) kinetic simulations in large or open-boundary systems have pointed out that the electron diffusion region does not remain compact and is elongated in the outflow direction, which leads to a bottleneck for the magnetic flux inflow and results in a drop in the reconnection rate [7,8]. The elongated electron diffusion region could be unstable in the current density direction, and anomalous resistivity due to wave-particle interactions is expected to enhance the magnetic dissipation in three-dimensional (3D) systems [8].

It has been known that cross-field kink modes are easily driven in a thin current sheet due to the cross-field ion flow, and can give rise to the magnetic dissipation via anomalous resistivity [9–11]. Historically speaking, the kink mode has been recognized as the drift kink instability (DKI) for low mass ratio ($m_i/m_e \lesssim 25$) [9, 10]. Although this instability results in a significant decrease in the growth rate for high mass ratio ($m_i/m_e > 100$) [12], the kink mode is still alive as the ion-ion kink instability and the linear properties are essentially identical to the DKI [13]. Furthermore, the kink structure of the current sheet has also been observed recently in the Earth's magnetotail and is sometimes accompanied by magnetic reconnection [14]. However, it is still an open question how the kink modes affect magnetic reconnection in 3D undriven systems.

In the present study, we examine 3D full kinetic simulations in a large system, in which magnetic reconnection evolves in association with a kink mode propagating in the cross-field direction. It is demonstrated that the kink mode provides a significant fraction of dissipation through an anomalous resistivity

author's e-mail: keizo@stelab.nagoya-u.ac.jp

in addition to the electron inertia resistivity, and enhances the reconnection rate so as to achieve the fast reconnection.

2. Simulation Model

The simulations are performed using an electromagnetic particle-in-cell (PIC) code with the adaptive mesh refinement and particle splitting-coalescence method [15]. We first consider a 3D system where the boundaries are periodic in the x and y directions, and conducting wall in the z direction. The simulations are carried out using a Harris-type current sheet with the magnetic field $B_x(z) = -B_0 \tanh(z/L)$ and the number density $n(z) = n_{ps}\,\mathrm{sech}^2(z/L) + n_b \tanh^2(z/L)$, where L is the half width of the current sheet. We choose $L = 0.5\lambda_i$ with λ_i the ion inertia length defined by n_{ps}, and $n_b = 0.044 n_{ps}$. Although there appears a weak pressure imbalance due to the background density profile, the equilibrium is quickly established without any significant modification to the current sheet structure. The system size is $l_x \times l_y \times l_z = 31\lambda_i \times 7.7\lambda_i \times 31\lambda_i$, which is covered with the base level cells of size $\Delta_{L_B} = 0.24\lambda_i$. The cells can be subdivided until the dynamic range level with $\Delta_{L_D} = 0.03\lambda_i$. The time step is $\Delta t\omega_{ci} = 1.6 \times 10^{-3}$ for all the cell levels and particles, with ω_{ci} the ion cyclotron frequency defined by B_0. The other parameters are $m_i/m_e = 25$, $c/V_A = 10$, $T_{i,ps}/T_{e,ps} = 5.0$, $T_{i,lobe}/T_{e,lobe} = 1.0$, and $T_{e,lobe}/T_{e,ps} = 1.0$, where $V_A = B_0/\sqrt{\mu_0 m_i n_{ps}}$ is the Alfvén velocity.

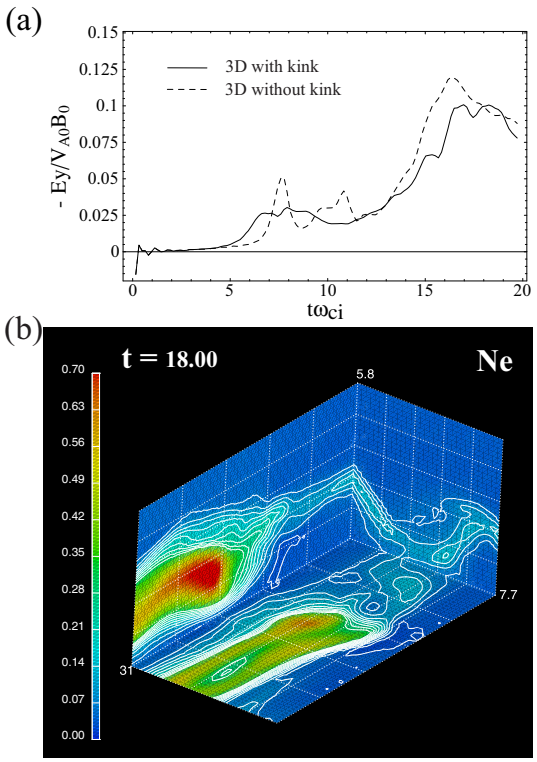

Fig. 1 (a) Time profiles of the reconnection electric field in the 3D simulations for the cases with the kink mode (solid curve) and without the kink mode (dashed curve). E_y is normalized by the upstream values and averaged over the initial X-line. (b) 3D structure of the kinked current sheet at $t\omega_{ci} = 18$. Color contours represent the profile of the electron number density, and white solid curves are its isolines.

3. Results

Magnetic reconnection is initiated with a small perturbation to the magnetic field, which produces the X-line along the current density at $(x, z) = (l_x/2, 0)$. This setup allows the tearing instability to grow on the same time scale as the kink mode. Note that the purpose of the present study is not to investigate the triggering mechanism of reconnection as discussed in Horiuchi and Sato [10]. The reconnection rate evaluated with $-E_y$ at the initial X-line grows very slowly until $t\omega_{ci} \simeq 5$ as shown in Fig.1a (solid curve), then one can see a sudden enhancement. This enhancement is due to the activity of the electrostatic mode of the lower hybrid drift instability (ES-LHDI), which is driven by the diamagnetic current at the edge of the current sheet, facilitating the onset of a fast reconnection [16]. However, the ES-LHDI quickly disappears around the X-line, as the convection flow associated with reconnection removes the plasma away from the vicinity of the X-line, so that the density gradient is significantly reduced. The subsequent mode arising in the cross-field direction is a kink mode, and persists until the end of the simulation. It is interesting to note that the kink mode still survives even when the plasma sheet ions, which initially has a drift velocity, are completely replaced around the X-line by the lobe ions with no initial drift velocity. This is because the lobe ions are accelerated in the cross-field direction due to the reconnection electric field within the ion-scale diffusion region and support the kink mode. Thus, the kink mode can coexist with magnetic reconnection (Fig.1b). The kink mode deforms drastically the structure of the current sheet and electron flow around the electron diffusion region. Nevertheless, the time profile of the reconnection electric field is almost identical to the run without the kink mode, and a fast magnetic reconnection with $-E_y \sim 0.1$ normalized by the upstream values is achieved. Here the run without the kink mode is carried out in the system with $31\lambda_i \times 1.9\lambda_i \times 31\lambda_i$, which allows the ES-LHDI to grow but is not large enough for the kink mode.

In order to investigate the dissipation mechanism responsible for the fast reconnection associated with the kink mode, we introduce a new coordinate system (x, y', z'), where the y' axis is parallel to the isoline of B_x. We consider the y' component of the generalized

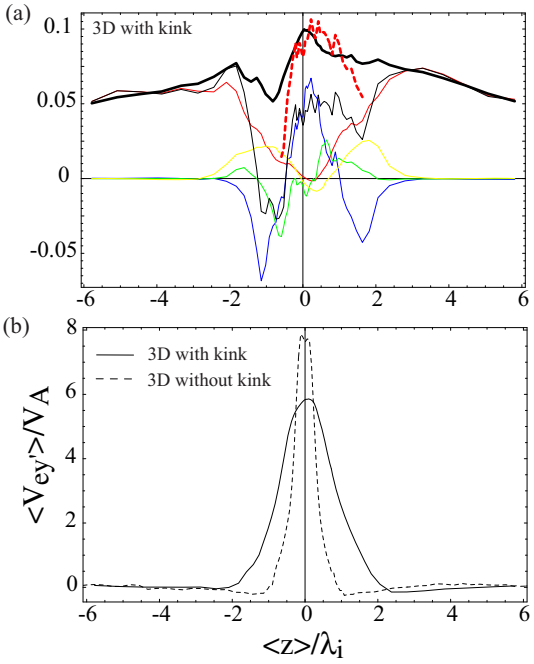

Fig. 2 (a) Results for the 3D simulation with the kink mode at $t\omega_{ci} = 18$. The profiles shown are taken through the X-line in the z' direction of the y' component of the generalized Ohm's law averaged over the y' direction. $\langle -E_{y'} \rangle$ is represented by black thick curve, $(1/\langle n_e \rangle)(\langle n_e \boldsymbol{V}_e \rangle \times \langle \boldsymbol{B} \rangle)_{y'}$ by red solid curve, $(1/e\langle n_e \rangle)\langle (\nabla' \cdot \boldsymbol{P}_e)_{y'} \rangle$ by blue curve, $(m_e/e\langle n_e \rangle)\langle n_e dV_{ey'}/dt \rangle$ by green curve, $(1/\langle n_e \rangle)\langle \delta n_e \delta E_{y'} \rangle$ by yellow curve, and sum of the right-hand side of Eq.(2) by black light curve. Red dashed curve presents the sum of the anomalous resistivity $\eta^{an}\langle j_{y'} \rangle$ and the right-hand side of Eq.(2). η^{an} is deduced from the 2D simulation with $m_i/m_e = 25$ at $t\omega_{ci} = 13$. On the horizontal axis, z averaged over the y' direction is employed. (b) Profiles of $\langle V_{ey'} \rangle$ through the X-line in the z' direction for the 3D simulations with the kink mode (solid curve) and without the kink mode (dashed curve).

Ohm's law averaged over the y' axis

$$\langle -E_{y'} \rangle = \frac{1}{\langle n_e \rangle}(\langle n_e \boldsymbol{V}_e \rangle \times \langle \boldsymbol{B} \rangle)_{y'} + \frac{1}{e\langle n_e \rangle}\langle (\nabla' \cdot \boldsymbol{P}_e)_{y'} \rangle + \frac{m_e}{e\langle n_e \rangle}\left\langle n_e \frac{dV_{ey'}}{dt} \right\rangle + \frac{1}{\langle n_e \rangle}\langle \delta n_e \delta E_{y'} \rangle , \quad (2)$$

where $\langle \cdot \rangle = (1/l_y)\int_0^{l_{y'}} \cdot dy'$ represents the average over the y' axis with $l_{y'}$ the path length along the integral interval, $\nabla' = (\partial/\partial x, \partial/\partial y', \partial/\partial z')$ is the nabla operator in the new coordinate, and δ denotes the perturbed value. The profiles for each term in the z' direction are shown in Fig.2a. As is the case without the kink mode [5], the electron pressure gradient term is dominant at the X-line, that is, at $\langle z \rangle \approx 0$. However, the amplitude is reduced compared to the case without the kink mode. This is because the kink mode broadens the current sheet, so that the peak of the electron bulk velocity becomes lower than the case without the kink mode (Fig.2b). Since the $\nabla \cdot \boldsymbol{P}_e$ term at the X-line is produced due to the meandering/Speiser motion of the electrons and originates from the electron inertia resistivity, the weaker electron acceleration results in the lower $\nabla \cdot \boldsymbol{P}_e$. Nevertheless, it is interesting that the reconnection electric field at the X-line is still large and a significant discrepancy arises between the electric field and $\nabla \cdot \boldsymbol{P}_e$ term.

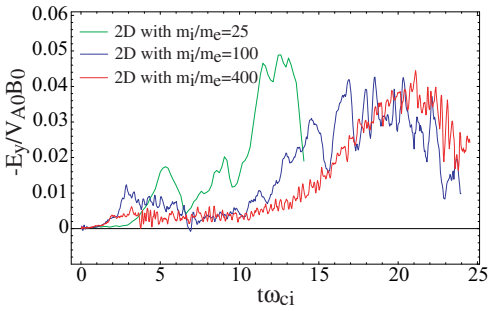

Fig. 3 Time profiles of $-E_y$ at the initial neutral sheet in the 2D simulations for the cases of $m_i/m_e = 25$ in green, 100 in blue, and 400 in red. E_y is normalized by the values at the initial lobe and is averaged over the initial neutral sheet.

In order to clarify the dissipation mechanism due to the kink mode alone in a system where magnetic reconnection is not incorporated, we next consider 2D simulations in the yz plane which is orthogonal to the magnetic field. In the 2D system, the particles accelerated in the current sheet are not easily ejected from the acceleration region, so that the inertia resistivity is excluded. The simulation parameters are the same as those for the 3D simulations except for the mass ratio. We examine three mass ratios: $m_i/m_e = 25$ with $\Delta_{L_B} = 0.24\lambda_i$ and $c/V_A = 10$, $m_i/m_e = 100$ with $\Delta_{L_B} = 0.12\lambda_i$ and $c/V_A = 20$, and $m_i/m_e = 400$ with $\Delta_{L_B} = 0.06\lambda_i$ and $c/V_A = 41$. In each of the runs, the kink mode evolves after the ES-LHDI saturates and eventually a large-scale kink structure with the wavelength $\lambda = l_y$ is formed. Fig.3 shows time evolutions of the electric field $-E_y$ at the initial neutral sheet, which is equivalent to the rate of magnetic dissipation. It is clear that magnetic dissipation is generated and associated with the kink mode. The amplitude is almost independent of the mass ratio, which indicates that the dissipation would persist even in the system with the real mass ratio $m_i/m_e = 1836$. The magnetic dissipation is produced through the anomalous resistivity which is caused by plasma heating, especially electron heating, via a wave-particle interaction. As the kink mode evolves, the electrons are strongly

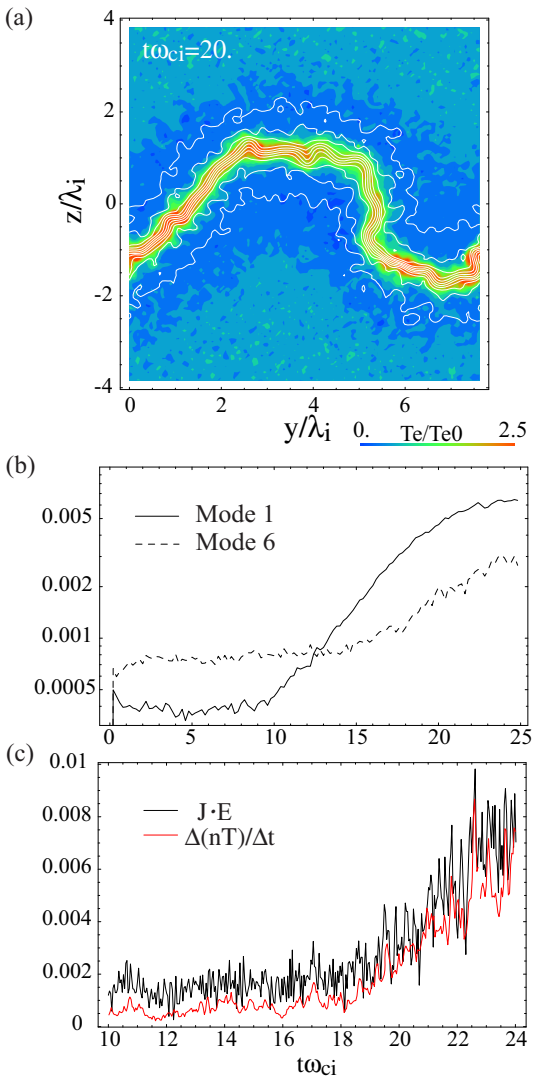

Fig. 4 Results for the 2D simulation with $m_i/m_e = 400$. (a) Snapshot at $t\omega_{ci} = 20$ of the electron temperature in color contours and isolines for B_x in white curves. Electron temperature is normalized by the initial temperature. (b) Time profiles of the Fourier amplitude of E_y averaged over the z direction for the mode 1 (solid curve) and mode 6 (dashed curve). (c) Time profiles of $\boldsymbol{j} \cdot \boldsymbol{E}$ in black curve and plasma heating rate $\partial(nT)/\partial t$ in red curve, averaged over the entire system.

heated in the thin current sheet (Fig.4a). The electrons are stochastically scattered and are effectively heated at the corner of "small bumps" embedded in the kink mode. The "small bumps" are generated due to a hybrid-scale kink mode recognized as the current sheet kink instability (CSKI) [11] or electromagnetic LHDI (EM-LHDI) [17], and have a characteristic scale $k\sqrt{\lambda_i\lambda_e} \sim 1$ with λ_e the electron inertia length. The large-scale kink mode also plays an important role in enhancing the heating rate, because it increases the total length of the thin current sheet. The evidence is clearly shown in Fig.4b and Fig.4c. The hybrid-scale kink mode with $k\sqrt{\lambda_i\lambda_e} \approx 1.1$ (mode 6) grows significantly after the onset of the large-scale kink mode (mode 1), coinciding with the plasma heating rate $\partial(nT)/\partial t$, where $nT = n_iT_i + n_eT_e$ is the total thermal energy. This indicates that the hybrid-scale kink mode is responsible for the plasma heating. In the 3D simulation in Fig.1b, because of small mass ratio and low plasma density, the expected scale of the hybrid-scale kink mode is comparable with the system size l_y. Thus, the "small bumps" are not clearly seen in the 3D run, instead, the electrons are scattered at the corner of the large-scale kink structure itself.

In order to generate the electrical resistivity, the bulk energy of the particles which are responsible for the current density has to be removed from the system due to some effective collision. Under a quasi-steady condition, the energy gain of the fluid plasma should be balanced with the energy loss due to the collisional effects, so that

$$\boldsymbol{j} \cdot \boldsymbol{E} \sim \frac{1}{2} n_i m_i V_{ic}^2 \nu_i + \frac{1}{2} n_e m_e V_{ec}^2 \nu_e, \tag{3}$$

where $\boldsymbol{j} = e(n_i\boldsymbol{V}_i - n_e\boldsymbol{V}_e)$ is the current density, ν_s the effective collision frequency of species s, and $\boldsymbol{V}_{sc} = 2\boldsymbol{V}_s$ the effective bulk velocity of species s just before the collision. If the effective collision converts the bulk energy to the thermal energy, the right-hand side of Eq.(3) should be balanced with the time derivative of the thermal energy

$$\boldsymbol{j} \cdot \boldsymbol{E} \sim \frac{\partial(nT)}{\partial t}. \tag{4}$$

This relation is verified in Fig.4c, which demonstrates that the energy gain of the plasma at each time is balanced with the growth rate of the thermal energy. Changes in the bulk energy for both the species are negligible. Since the inertia resistivity is not effective in the 2D system, the anomalous resistivity is simply written in the form $\eta^{an} = \left\langle -E_{y'}^{(2D)} \right\rangle / \left\langle j_{y'}^{(2D)} \right\rangle$. We deduce the contribution of the anomalous resistivity in the 3D system by adopting η^{an} in the 2D system with $m_i/m_e = 25$, which leads to the form $\left\langle -E_{y'}^{an} \right\rangle = \left(\left\langle j_{y'}^{(3D)} \right\rangle / \left\langle j_{y'}^{(2D)} \right\rangle \right) \left\langle -E_{y'}^{(2D)} \right\rangle$. In Fig.2a (red dashed curve), the sum of $\left\langle -E_{y'}^{an} \right\rangle$ and the right-hand side of Eq.(2) is plotted in the vicinity of the X-line. It is shown that the anomalous resistivity greatly enhances the magnetic dissipation and makes a significant contribution for realizing the fast reconnection, compensating the reduction in the inertia resistivity.

4. Conclusion

We have shown that a kink mode excited in the cross-field direction significantly contributes to the fast reconnection in 3D undriven system, providing magnetic dissipation through the anomalous resistivity. The dissipation mechanism is very different from

2D reconnection without the kink mode, where the fast reconnection is supported by the inertia resistivity alone. The anomalous resistivity is produced by the electron heating within the thin electron current sheet. Such an electron heating due to electromagnetic fluctuations is also observed in laboratory experiment during fast reconnection [e.g., [18]]. It is interesting that, although the kink mode broadens the width of the current sheet and decreases the inertia resistivity, the anomalous resistivity compensates the depletion so as to keep the high reconnection rate. The present result suggests that the electron dynamics in the electron diffusion region is automatically adjusted so as to produce sufficient dissipation for the fast reconnection.

This work has been partly supported by a collaborative research project at STE Laboratory, Nagoya University, by the Grant-in-Aid for Research Fellows of the JSPS, and by the Natural Sciences and Engineering Research Council of Canada. Simulations were performed by the Fujitsu PRIMEPOWER HPC2500 at Nagoya University and Kyoto University.

[1] S.-I. Akasofu, Planet. Space Sci. **12**, 273 (1964).
[2] P. A. Sweet, Ann. Rev. Astron. Astrophys. **7**, 149 (1961).
[3] T. W. Speiser, Planet. Space Sci. **18**, 613 (1970).
[4] M. Tanaka, Phys. Plasmas **2**, 2920 (1995).
[5] H. J. Cai and L. C. Lee, Phys. Plasmas **4**, 509 (1997).
[6] J. Birn *et al.*, J. Geophys. Res. **106**, 3715 (2001).
[7] W. Daughton *et al.*, Phys. Plasmas **13**, 072101 (2006).
[8] K. Fujimoto, Phys. Plasmas **13**, 072904 (2006).
[9] M. Ozaki *et al.*, Phys. Plasmas **3**, 2265 (1996).
[10] R. Horiuchi and T. Sato, Phys. Plasmas **6**, 4565 (1999).
[11] I. Shinohara *et al.*, Phys. Rev. Lett. **87**, 095001 (2001).
[12] W. Daughton, Phys. Plasmas **6**, 1329 (1999).
[13] H. Karimabadi *et al.*, J. Geophys. Res. **108**, 1400 (2003).
[14] T. V. Laitinen *et al.*, Ann. Geophys. **25**, 1025 (2007).
[15] K. Fujimoto and R. D. Sydora, Comput. Phys. Comm. **178**, 915 (2008).
[16] M. Scholer *et al.*, Phys. Plasmas **10**, 3521 (2003).
[17] W. Daughton, Phys. Plasmas **10**, 3103 (2003).
[18] H. Ji *et al.*, Phys. Rev. Lett. **92**, 115001 (2004).